BLUE COMPACT DWARFS AT z$\lesssim$1: IMPLICATIONS FOR GALAXY EVOLUTION AND THE STAR FORMATION HISTORY OF THE UNIVERSE

R. Guzmán [1] & D. C. Koo [2]

[1] *Dept. of Astronomy, Yale University, 260 Whitney Ave., New Haven, CT 06520, USA.*

[2] *UCO/Lick Observatory, UCSC, Santa Cruz, CA 95060,USA.*

Abstract

We study the nature of faint blue compact galaxies (BCGs) at redshifts $z \sim 0.2 - 1.3$. Most distant BCGs have masses $M \lesssim 10^{10} M_{\odot}$, i.e., they are *dwarf* stellar systems. The majority of these galaxies have colors, sizes, surface brightnesses, luminosities, velocity widths, excitations, star formation rates (SFR), and mass-to-light ratios characteristic of nearby young HII galaxies. The more massive BCGs form a more heterogeneous class of evolved starbursts, similar to local disk starburst galaxies. Without additional star formation, HII-like BCGs will most likely fade to resemble today's spheroidal galaxies such as NGC 205. From the comparison with the global comoving SFR densities derived from previous data sets, we conclude that BCGs, though only ~20% of the general field population, may contribute as much as ~45% to the global SFR density of the universe at $z \lesssim 1$.

1 Introduction

One of the major goals in modern cosmology is to unveil the star formation history of the universe. It seems now well-accepted that the global SFR density of the universe increases with lookback time by a factor of ~10 at redshift $z \sim 1$ ([2],[14],[17]). An important remaining question is: what is the nature of the galaxy population responsible for this increase of the star formation activity in the last ~8 Gyrs?. This population may be closely related to the numerous faint blue galaxies observed in deep images of the sky, whose nature remains a controversial issue (see reviews by [13],[4]) and references therein). The high surface density and weak clustering of these galaxies argue against their being either the progenitors or the merging components of present-day bright galaxies ([14],[3]). Various theoretical scenarios have instead suggested that the faint blue galaxies are low-mass stellar systems experiencing their initial starburst at redshifts $z \leq 1$, some of which turn into the present population of spheroidal galaxies (Sph), such as NGC 205 ([1]).

In this project we investigate the nature of a subset of faint blue galaxies characterized by being very compact. The "compactness" criterion optimizes the selection of objects that are most likely to be low-mass starbursts. The goals are: to identify their local counterparts, to assess their evolution with look-back time, and to study their role on the star formation history of the universe. A full description of the results summarized here can be found in [11],[12],[8],[9],[10], and [21]. Unless specified otherwise, we adopt $H_0 = 50$ km s^{-1} Mpc^{-1} and $q_0 = 0.05$.

2 The Data

The main galaxy sample consists of 45 compact emission-line galaxies selected from I_{814} HST images of the flanking fields (FF) around the Hubble Deep Field (HDF; [25]). These objects are faint (I_{814} <23.74) and compact in the sense that they have small apparent half-light radii ($r_{1/2} \leq 0.5$ arcsec) and high surface brightnesses ($\mu_{I814} \leq 22.2$ mag arcsec^{-2}). Spectra for these objects were obtained using LRIS at the Keck telescope with a slitwidth of 1.1 arcsec and a 600 l/mm grating. The effective resolution is ∼3.1 Å FWHM. Typical exposure times were 3000s. The total spectral range is ∼4000-9000 Å. We also obtained two 300s direct V-band exposures with LRIS in order to derive colors. This sample is used to study the general properties of this galaxy class and to investigate their role in the star formation history of the universe.

In addition to the FF sample, we have studied in detail 12 compact narrow emission-line galaxies (CNELGs) selected from [19]. For each of these objects, we obtained echelle spectra using HIRES at the Keck telescope with a resolution of 0.13 Å FWHM. The high spectral resolution provides information not only about their velocity widths but also about their line profiles. Structural parameters for all these galaxies were measured from HST images. Detailed morphology and color structure for 5 such objects were determined from V_{606} and I_{814} images taken with the Planetary Camera. This overall higher quality data set is used to investigate the evolution of this galaxy class from their lookback times till the present.

The final data set for both galaxy samples includes: redshifts, colors, absolute blue magnitudes (M_B), half-light radii (R_e), average surface brightnesses within R_e (SB_e), velocity widths (σ), masses (M), mass-to-light ratios (M/L), O[III]/Hβ line ratios (for objects at $z \lesssim 0.7$), and SFRs.

3 The Nature of Blue Compact Galaxies at $z \lesssim 1$

The spectra of distant compact emission-line galaxies exhibit prominent oxygen and Balmer emission lines and blue continua characteristic of vigorous star-forming systems and narrow-line active galaxies (Figure 1a). Most of these objects are bluer than a typical Sbc galaxy (Figure 1b). Hereafter, we refer to this galaxy class as blue compact galaxies (BCGs). For convenience, we divide the sample into intermediate-redshift ($z < 0.7$) and high-redshift ($z > 0.7$) samples.

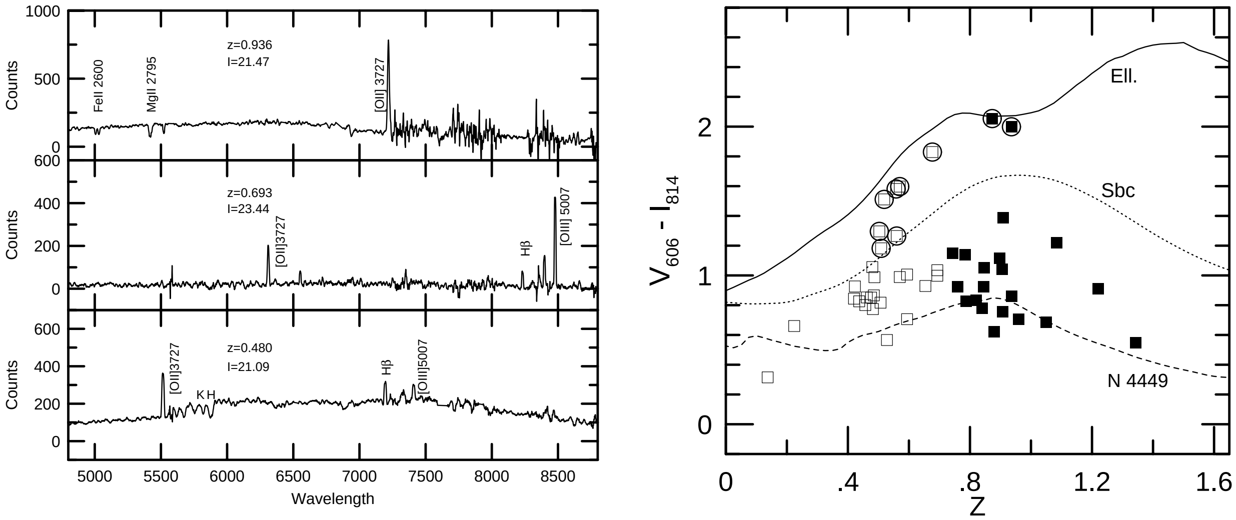

Figure 1: (a) Example of Keck spectra of distant BCGs. (b)$V_{606} - I_{814}$ color as a function of redshift. The tracks of local elliptical, Sbc and starburst (NGC 4449) galaxies are based on observed SEDs (no color evolution). Objects with absorption-line dominated spectra -not included in this study- are marked with ($\circ$).

Global structural galaxy properties can be adequately described using the $SB_e - M_B$ and $R_e - \sigma$ diagrams ([7]). In these diagrams, various galaxy types define distinct correlations, albeit with large scatter (Figures 2a and 2b). Most of our BCGs follow the sequences defined by young starbursts, such as nearby HII galaxies. Despite having luminosities around L^*, most BCGs are *dwarf* stellar systems with masses $M \lesssim 10^{10} M_\odot$.

To parametrize the starburst properties of BCGs we use the $M_B - [OIII]/H\beta$ and the $M - SFR/M$ diagrams (Figures 3a and 3b). These diagrams discriminate among various types of starburst and active galaxies. Most BCGs with $[OIII]/H\beta$ measurements lie in the moderate to high excitation regime populated by nearby HII galaxies. These objects also have SFR/M characteristic of HII galaxies. A second group of distant BCGs have $[OIII]/H\beta$ and SFR/M similar to those of more evolved disk starbursts such as local DANS and SBNs. We have thus classified the BCG sample into HII-like and disk starburst-like galaxies, depending on their SFR/M (see Figure 3b). With this simple criterion, we find that ~60% of distant BCGs have global properties consistent with those of nearby HII galaxies, while the remaining 40% are similar to more evolved disk starbursts (see Table 1).

Table 1. Average Global Properties of distant BCGs

Class	M_B (mag)	SB_e (mag arcsec^{-2})	R_e (Kpc)	σ (km s^{-1})	M (10^{10}M$_\odot$)
HII-like	-20.0 ± 0.3	20.1 ± 0.4	2.2 ± 0.4	55 ± 6	0.4 ± 0.2
disk SB-like	-20.0 ± 0.3	20.9 ± 0.4	3.3 ± 0.4	87 ± 14	1.3 ± 0.2
Class	log SFR/M (10^{11} yr^{-1})	M/L (M/L)$_\odot$	$EW([OII])$ (Å)	$[OIII]/H\beta$	log $L_{H\beta}$ (ergs s^{-1})
HII-like	1.7 ± 0.1	0.3 ± 0.1	58 ± 8	2.9 ± 0.5	40.9 ± 0.1
disk SB-like	0.9 ± 0.1	1.0 ± 0.1	31 ± 7	2.1 ± 0.4	40.5 ± 0.1

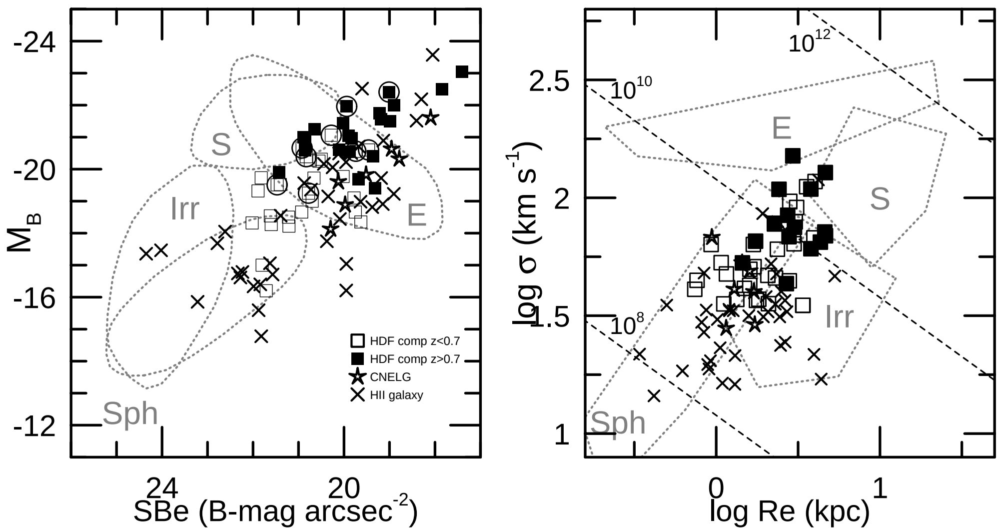

Figure 2: (a): SB_e vs. M_B. Dotted lines indicate the regions typically occupied by different classes of local galaxies. Nearby HII galaxy sample (crosses) is from [24]. (b): R_e vs. σ. Dashed lines represent constant-mass lines in $M_\odot$, estimated using the Virial Theorem.

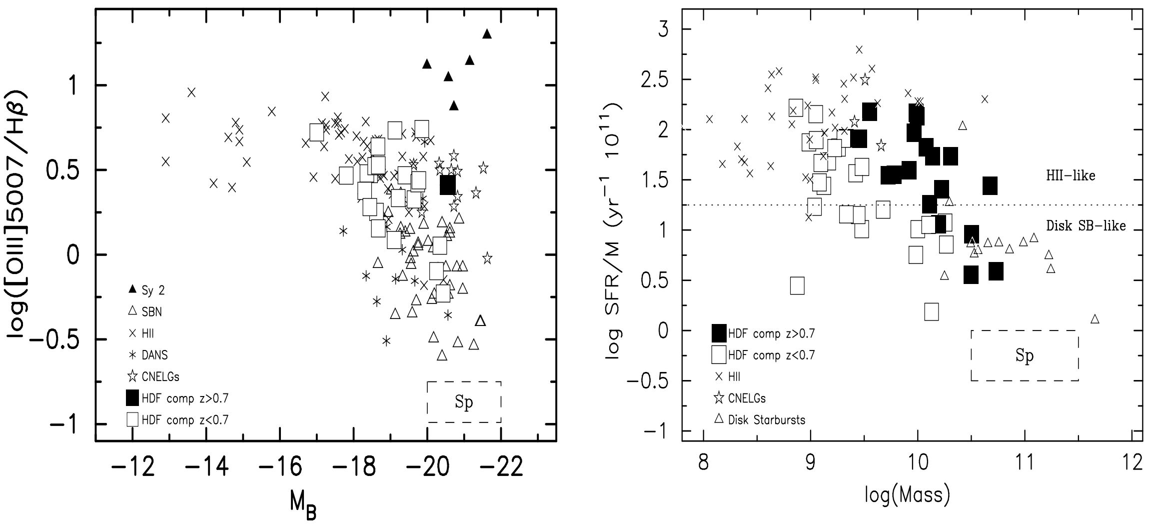

Figure 3: (a): M_B vs. $[OIII]/H\beta$. Local galaxy sample is from [6]; DANS: Dwarf Amorphous Nuclear Starbursts; SBN: Starburst Nuclei; Sy2: Seyfert 2 galaxies; HII: HII galaxies. Dashed lines represent the approximate location of spiral galaxies. (b): M vs. SFR/M. The dotted line represents the division between HII-like and disk starburst-like galaxies adopted in our classification.

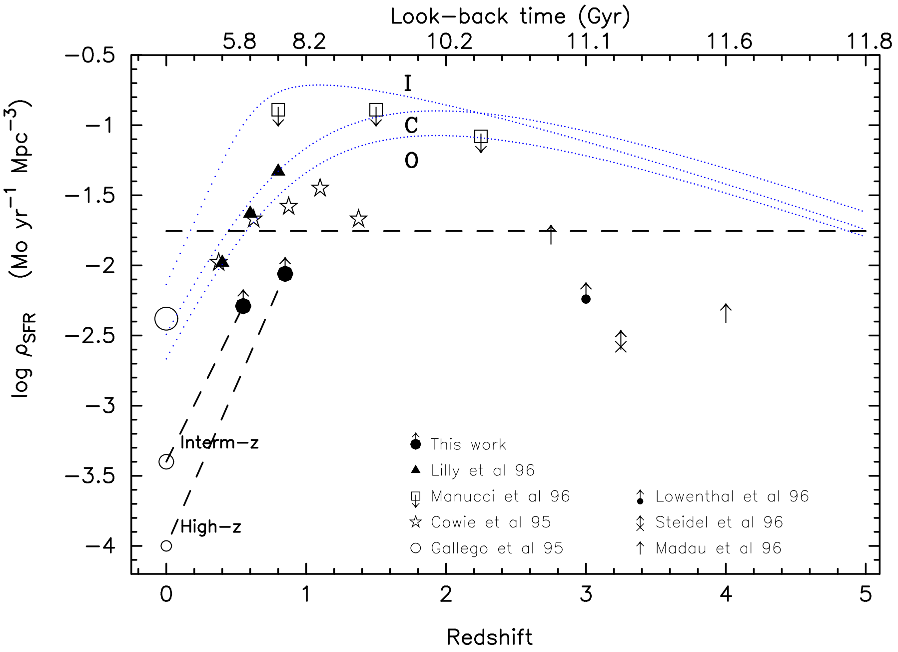

Figure 4: SFR density vs. redshift. Filled circles are the estimates for our BCG sample. These values should be compared to the open circles labelled "Interm-z" and "High-z, which represent the values for *similar* samples of nearby BCGs. Dotted lines represent Pei & Fall's models (1995). The dashed line represents the fiducial value. We adopt $H_0 = 50$ km s^{-1} Mpc^{-1} and $q_0 = 0.5$.

4 Implications for the Star Formation History of the Universe

The $M - SFR/M$ diagram shown in Figure 3b suggests two other interesting results. First, the highest values of the SFR/M exhibited by compact galaxies are similar to those of local HII galaxies. Thus we do not find evidence for an increase in the peak of the SFR/M activity with redshift in our sample. Second, BCGs at $z > 0.7$ are, on average, $\sim$10 times more massive than their counterparts with similar SFR/M at $z < 0.7$. Although selection effects may account for the lack of low-mass BCGs at high-z, they cannot explain why the more massive star-forming systems are not present in the intermediate-z sample. This is not the result of a volume-richness effect either, since the volumes mapped in both samples differ by only a factor $\sim$ 1.5. This result thus suggests a significant *increase in the number of more massive star-forming galaxies with redshift*, although this result should be taken with caution given the small number of galaxies involved in this analysis.

To investigate the contribution of BCGs to the star formation activity of the universe at $z \lesssim 1$, we consider our sample in the context of the current picture of the evolution of the SFR density with redshift. This picture is summarized in Figure 4. The interpretation of this figure should be approached with caution, given the likely differences in the calibrations for the various SFR tracers, incompleteness of the data sets, and uncertainties in the models (see Madau, this conference, for a detailed discussion of this figure). Despite these caveats, it seems now well-accepted that the total SFR density of the universe decreased by a factor of $\sim$10 from $z \sim 1$ to the present-day. Assuming our sample is representative of the general population of BCGs, we estimate that the total SFR densities associated to this class are: 0.004 $M_\odot$ yr^{-1} Mpc^{-3} at z=0.55, and 0.008 $M_\odot$ yr^{-1} Mpc^{-3} at z=0.85. These values, when compared to a

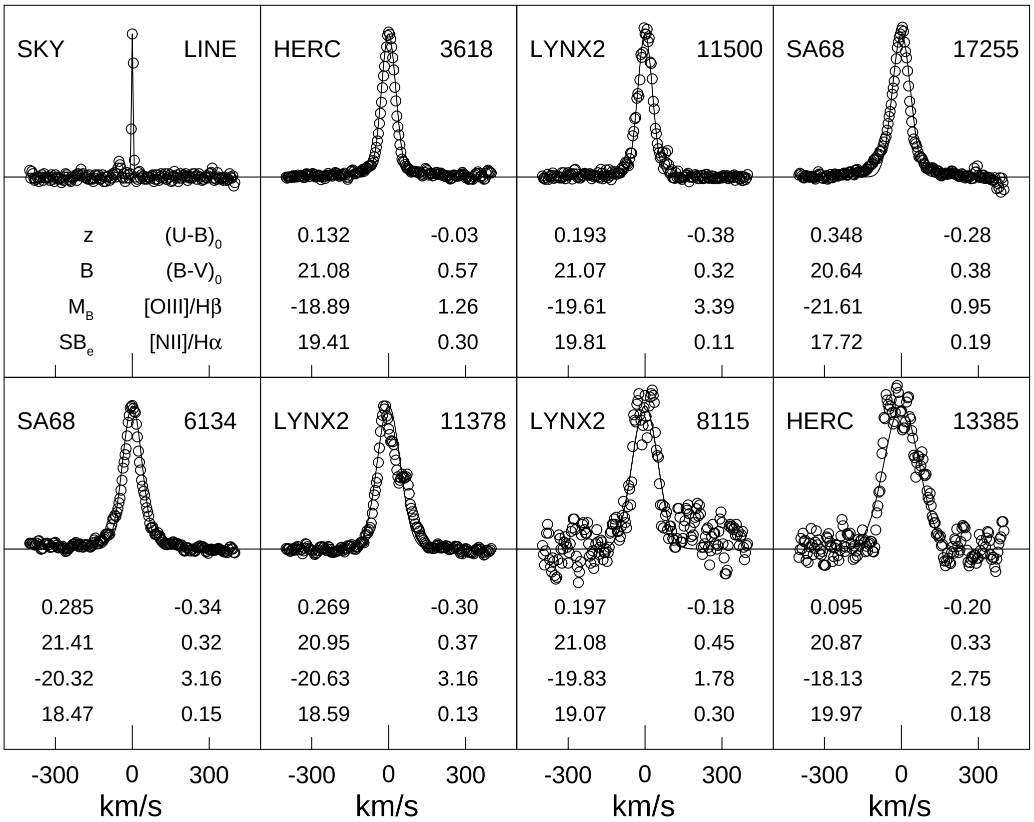

Figure 5: [OIII]λ5007 emission line profiles in BCGs. Velocity widths for these objects range from $\sigma = 28$ km s^{-1} (Herc-3618) to $\sigma = 68$ km s^{-1} (Herc-13385).

similar sample of local galaxies, support a similar decline of the SFR density in the last $\sim$8 Gyrs. From the comparison with the SFR densities derived by [2], we conclude that compact emission-line galaxies, though only $\sim$20% of the general field population, may contribute as much as $\sim$45% to the global SFR of the universe at $0.4 < z < 1$.

5 Implications for Galaxy Evolution

One of the most useful tools to study how distant young galaxies relate to nearby evolved stellar systems is the $R_e - \sigma$ diagram, since neither R_e nor σ depend strongly on the luminosity evolution of the stellar population. In this section, we focus the discussion on a sample of 12 BCGs with the best quality σ and R_e data. These galaxies were selected from a larger sample of compact narrow emission line galaxies (CNELGs) which have global properties consistent with those characteristic of the HII-like BCG galaxy class described in Section 3. Figure 5 shows a representative example of the emission lines used to measure σ for this sample. Note that the line profiles are adequately fitted by a Gaussian, suggesting that the broadening of the emission lines may be due to random gas motions rather than bulk rotation. Figure 6 summarizes the results of our detailed study of their morphology and color structure.

In Figure 7a, we show the $R_e - \sigma$ diagram for these 12 HII-like BCGs. Although there are several physical processes that may modify R_e and σ during galaxy evolution (see Figure 7a), we find no evidence against the idea that HII-like BCGs are related structurally and kinematically

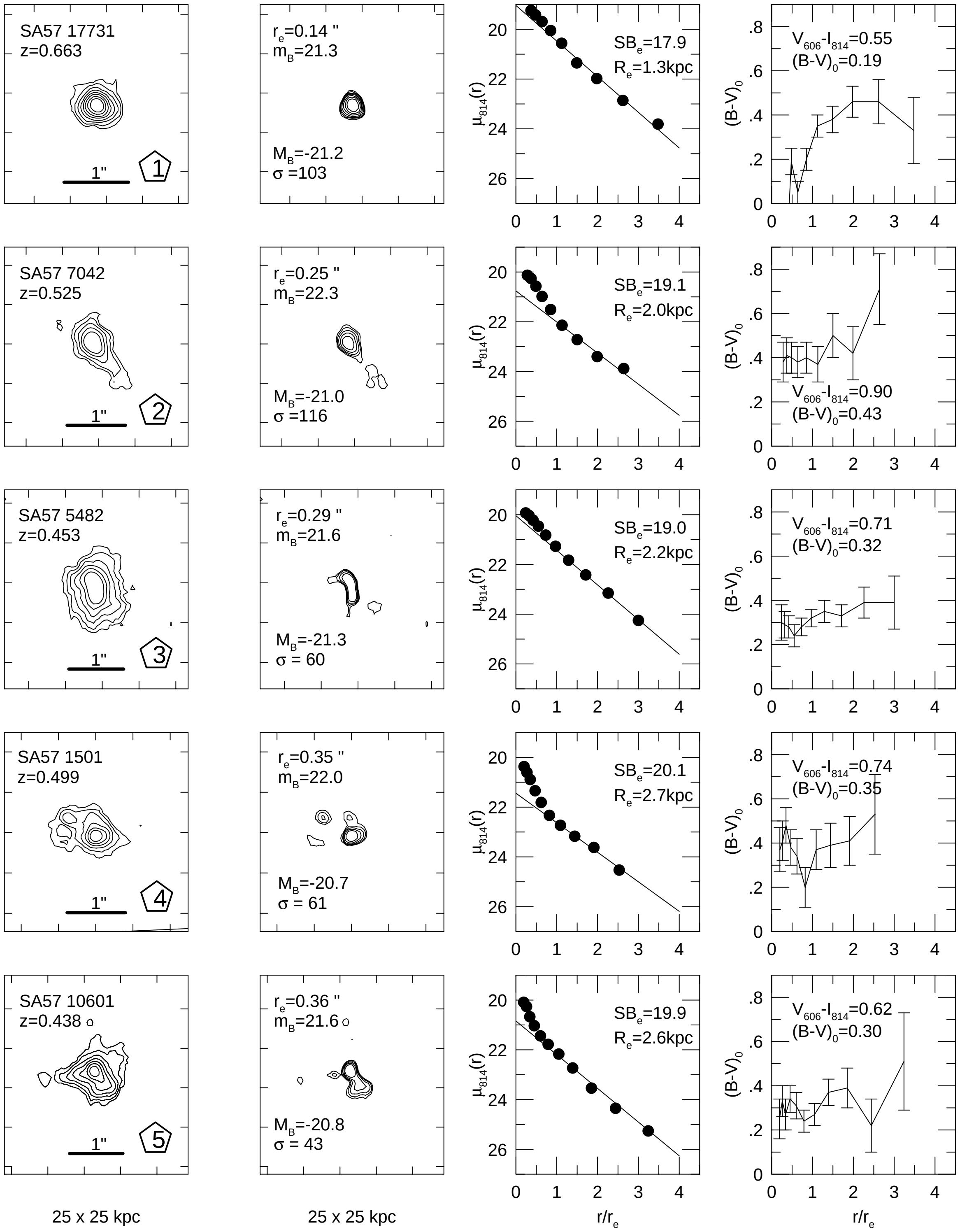

Figure 6: This figure shows four panels for each galaxy. The first panel is the V_{606} galaxy contour map in 0.5 mag intervals. The outermost contours correspond to 0.5 mag above sky level (i.e., $V_{606} \sim 23$ mag arcsec^{-2}). The contours are slightly smoothed, typically block-averaged by 3×3 pixels. The size of the panel is 25×25 kpc while the horizontal scale represents 1 arcsec. The second panel shows the residual contour maps of the bluer, higher surface brightness component (i.e., the starburst) after the underlying, exponential-like component has been removed. The third panel shows the I_{814} surface brightness profiles $\mu(r)$. The size of the data points is representative of the typical uncertainty in our measurements. The fourth panel shows the rest-frame $(B - V)$ color gradient.

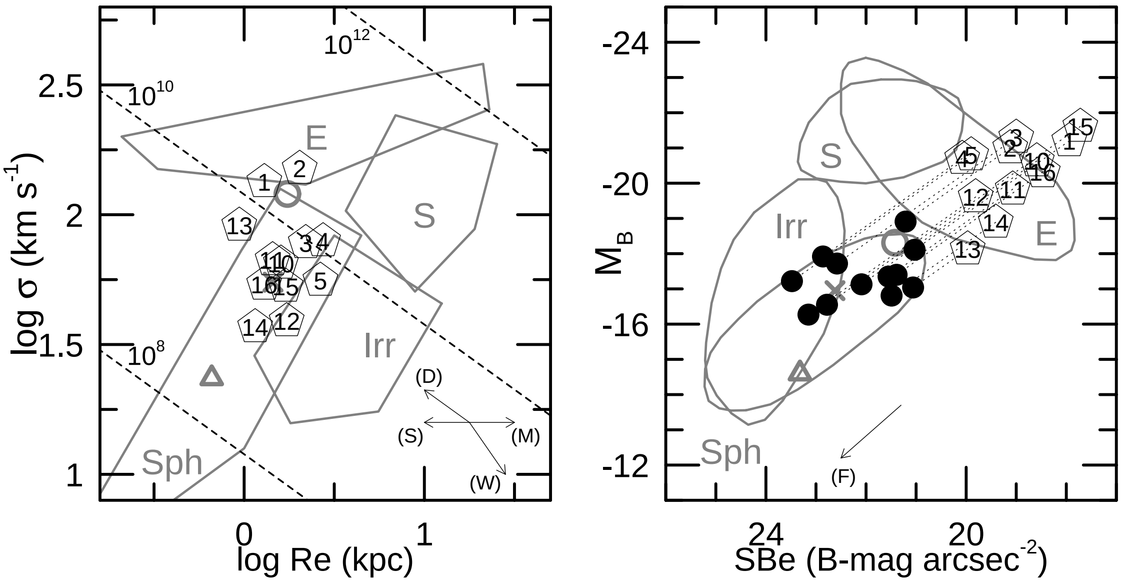

Figure 7: (a) log R_e vs logσ for HII-like BCGs. Point symbols with no labels represent the values of three typical spheroidal galaxies (NGC 147: triangle; IC3393: cross; NGC 3605: circle). The arrows represent the effect of dissipation (D), mergers (M), stripping (S) and galactic winds (W) on R_e and σ. (b) SB_e vs M_B. Point symbols as before. The arrow (F) represents the direction of fading. Dotted lines show the predicted luminosity evolution for each galaxy from its look-back time till the present. Filled circles represent the final faded positions.

to the nearby dwarf galaxy population of Sph and Irr galaxies, rather than to giant systems such as E and Sp galaxies.

The evolution of HII-like BCGs into one galaxy class or the other may depend critically on their ability to retain part of the interstellar medium. Their extremely low M/L ratios suggest that the kinetic energy supplied by the current starburst is likely to be large enough, compared to the binding energy, to blow out most of the gas in galactic winds, halting thus the star-forming process. Without additional star formation they will fade within a few billion years. The total amount of fading will depend on the age/strength of the current burst *and* the extent of any underlying older population.

Although it seems reasonable to expect that the current burst may be the last *major* star-forming episode, it is likely that it was not the only burst of star formation. Indeed, BCGs show evidence for an older underlying population characterized by a lower surface brightness exponential profile and slightly redder colors than the starburst region. Using the $M/L-(B\text{-}V)$ diagram and [22]'s models (Figure 8), we estimate that the current starburst in BCGs may be, typically, $\lesssim$0.5 Gyrs old, and represent only $\sim$10% of the total galaxy mass. Assuming these burst parameters, the models predict that HII-like BCGs will fade by $\lesssim$4 mag from their lookback times till the present. Figure 7b shows the predicted position of the faded BCGs in the $SB_e - M_B$ diagram. After fading, BCGs would have the same low blue luminosities and surface brightnesses charateristic of the brightest Sph galaxies. We thus conclude that HII-like BCGs are most likely the progenitors of today's bright Sph galaxies such as NGC 205.

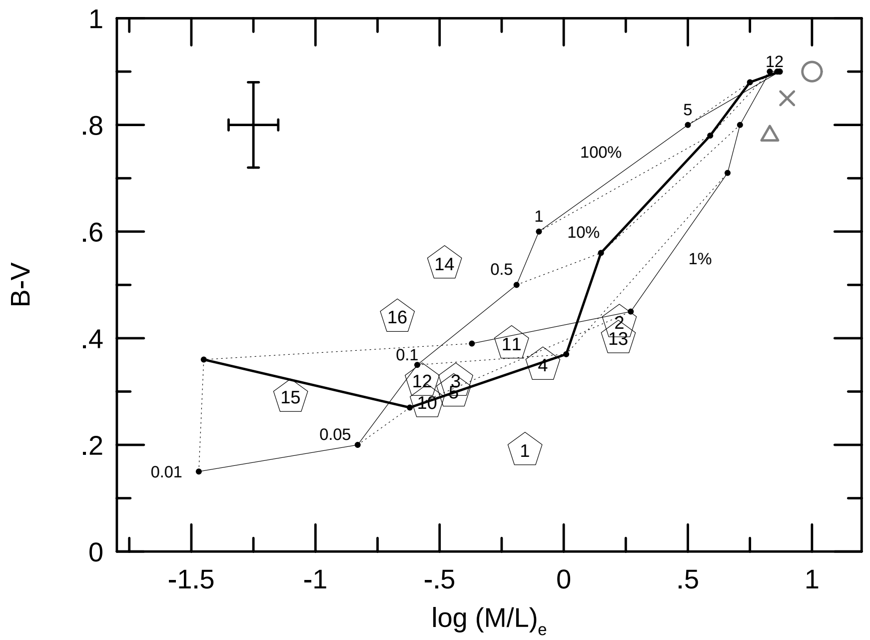

Figure 8: log $(M/L_B)_e$ vs $(B-V)$. Solid lines represent the model predictions for the evolution of a typical Sph galaxy after a single initial burst of star formation, and after a second burst involving 1% and 10% (thick solid line) of the total galaxy mass. Dots in the model lines correspond to ages 0.01, 0.05, 0.1, 0.5, 1, 5, and 12 Gyrs. The error bar represents the typical uncertainty in our measurements.

Acknowledgements. This project is a collaborative effort of the DEEP team at UC Santa Cruz (http://www.ucolick.org/∼deep/home.html). In particular, we thank Drew Phillips, Jesús Gallego, Anne Jangren, Matt Bershady, James Lowenthal, and Luc Simard for their significant contribution to this work. R. Guzmán would like to thank the organizing and scientific committees for their kind invitation and financial support to participate in this excellent meeting. Funding for this project is credited to NASA grants AR-06337.08-94A, AR-06337.21-94A, GO-05994.01-94A, AR-5801.01-94A, and AR-6402.01-95A from the Space Telescope Institute, and NSF grants AST 91-20005 and AST 95-29098. R. Guzmán also acknowledges partial support from the Hubble Fellowship grant HF-01092.01-97A.

References

[1] Babul A. & Ferguson H.C., 1996, ApJ, 458, 100

[2] Cowie L.L., Songaila A. & Hu E.M., 1991, Nature, 354, 460

[3] Efstathiou G., Berstein G., Katz, N. et al. , 1991, ApJ, 380, L47

[4] Ellis R.S., 1996, in ESO Workshop on *The Early Universe with the VLT*, in press

[5] Gallego J., Zamorano J., Aragón-Salamanca A. & Rego M., 1995, ApJ, 455, L1

[6] Gallego J., Zamorano J., Rego M. & Vitores A.G., 1997, ApJ, 475, 502

[7] Guzmán R., Lucey J.R., & Bower R.G., 1993, MNRAS, 265, 731

[8] Guzmán R., Koo D.C., Faber S.M. et al. , 1996, ApJ, 460, L5

[9] Guzmán R., Gallego J., Koo D.C. et al. , 1997, ApJ, 489, 559

[10] Guzmán R., Jangren A., Koo D.C. et al. , 1998, ApJ, 495, L13

[11] Koo D.C., Bershady, M.A., Wirth, G.D. et al. 1996, ApJ, 460, L5

[12] Koo D.C., Guzmán R., Faber S.M. et al. , 1995, ApJ, 440, L49

[13] Koo D.C., 1996, in IAU Symp. 168, ed. M. Kafatos (Dordrecht: Kluwer), p 201

[14] Lilly S.J., Cowie L.L. & Gardner J.P., 1991, ApJ, 369, 79

[15] Lilly S.J., Le Fevre O., Hammer F. & Crampton D., 1996, ApJ, 460, L1

[16] Lowenthal J.D., Koo D.C., Guzmán R. et al. 1997, ApJ, in press

[17] Madau P., Ferguson H.C., Dickinson M.E. et al. , 1996, MNRAS, 283, 1388

[18] Mannucci F., Thompson D. & Beckwith S.V.W., 1996, in *HST and the High Redshift Universe*, 37th Herstmonceux Conf., Cambridge, in press

[19] Munn J.A., Koo D.C., Kron R.G. et al. , 1997, ApJS, 109, 45

[20] Pei Y.C. & Fall S.M., 1995, ApJ, 454, 69

[21] Phillips A.C., Guzmán R., Gallego J. et al. , 1997, ApJ, 489, 54

[22] Schmidt A.A, Alloin D. & Bica E., 1995, MNRAS, 273, 945

[23] Steidel C.C., Giavalisco M., Pettini M. et al. , 1996, ApJ, 462, L17

[24] Telles E. & Terlevich R., 1997, MNRAS, 286, 183

[25] Williams R.E. et al. 1996, AJ, 112, 1335